Excellent Stability of Perovskite Solar Cells Encapsulated With Paraffin/ Ethylene-Vinyl Acetate/Paraffin Composite Layer

Biyu Long[1], Xianzi Zhou[2], Huafeng Cao[3], Renjie Chen[1], Nannan He[1], Lina Chi[2], Penghui Fan[4] and Xiaohong Chen[1]*

[1]Engineering Research Center for Nanophotonics & Advanced Instrument, Ministry of Education, School of Physics and Electronic Science, East China Normal University, Shanghai, China, [2]Beijing Smartchip Microelectronics Technology Co., Ltd., Beijing, China, [3]State Grid Gansu Electric Power Co., Lanzhou, China, [4]Beijing Smartchip Semiconductor Technology Co., Ltd., Beijing, China

Superior encapsulation technology is important for PSCs to prolong their lifetime and realize their commercial application. Paraffin/EVA/paraffin composite encapsulated layers were fabricated with the ambient environment under the thermal temperature of 80°C, which has advantages for simple procedures and low cost. PSCs encapsulated with paraffin/EVA/paraffin and pure EVA layers maintained 95 and 45% of the initial power conversion efficiency (PCE) aged for 1000 h at RH 75%, respectively. Paraffin/ EVA/paraffin-encapsulated PSCs were immersed in water for 5 h, which remained 98% of the original PCE, which is far superior to EVA-encapsulated PSCs. High melting point paraffin at 68°C shows better encapsulation than low melting point (60 and 55°C) paraffin, indicating that the high molecular weight of paraffin helps improve the encapsulation performance of PSCs. PSCs encapsulated with paraffin/EVA/paraffin showed better stability of Voc than pure EVA layer because paraffin can inhibit defects, voids, and edges of metal electrodes that quickly expand, and decay. Therefore, paraffin/EVA/paraffin combination encapsulation is an effective strategy, which can form continuous and dense hydrophobic composite encapsulation films with a friendly metal electrode.

Keywords: perovskite solar cells, encapsulation, stability, paraffin, eva

INTRODUCTION

Organic–inorganic hybrid perovskite solar cells (PSCs) have attracted great attention because of their excellent properties such as high optical absorptivity (van der Stam et al., 2017), adjustable energy band structure (Filip et al., 2014), high hole/electron transport mobility (Xing et al., 2013), long carrier diffusion length (Stranks et al., 2013), and low recombination rate (Ponseca et al., 2014), which help obtain high power conversion efficiency (PCE). The PCEs of PSCs have greatly increased and reached 25.5% in 2021 (Min et al., 2021), which is comparable to crystalline silicon solar cells. In addition, the simple preparation process compared to silicon solar cells (Liu and Kelly, 2014), has an obvious advantage in reducing the industrial application cost (Jeon et al., 2018). However, PSCs are sensitive to temperature, humidity, and ultraviolet light, which can greatly reduce the stability of PSCs (Tiep et al., 2016; Asghar et al., 2017; Zhang et al., 2018).

At present, some efficient strategies such as interface modification and doping, adjusting perovskite composites, using stable electron/hole transport material, and optimizing structures of PSCs have been demonstrated to improve the stability and PCEs of PSCs(Babaei et al., 2020; Lin, 2020; Zheng et al., 2020; Chen X. et al., 2021). Although developing the intrinsic performance of PSCs can greatly improve their stability, PSCs compared to silicon solar cells are still easily deteriorated by moisture, oxygen, heat, and ultraviolet light due to their properties, which require more strictly encapsulating technology (Chen Z. et al., 2021; Mazumdar et al., 2021).

Many encapsulation methods of PSCs have been developed and greatly prolong the lifetime of PSCs (Li et al., 2021). Atomic layer deposition (ALD) as a kind of potential encapsulation method of organic and flexible electronics (Zardetto et al., 2017; Ramos et al., 2018; Singh et al., 2020) has been applied to PSCs, which can improve the stability of PSCs. However, the ALD complex process and its expensive equipment limit its industrial application (Uddin et al., 2019). Using thermo-setting polymers such as ethylene-vinyl acetate (EVA) (Kempe et al., 2007), epoxy (EP), thermoplastic polyurethanes (TPU), polyurethane (PU), and UV-curable adhesive (UVCA) (Kim et al., 2012; Shi et al., 2017; Fu et al., 2019; Raman et al., 2021; Ma et al., 2022) as encapsulation materials have advantages of low cost and simple procedures, especially EVA polymers have been widely applied to commercial silicon solar cells. However, its moisture and oxygen resistance (Corsini and Griffini, 2020) cannot meet the strict requirement of PSCs because organic–inorganic perovskite material compared to silicon is more fragile (Asghar et al., 2017; Liu et al., 2019; Mohammadi et al., 2021).

In this study, the composite encapsulation layer based on cheap EVA and paraffin materials has been developed and applied to PSCs. Paraffin has an excellent hydrophobicity, chemical inertness, and ductility material (Krupa et al., 2007; Alkan et al., 2011) and can well offset the disadvantage of the EVA layer, which greatly improves the moisture and oxygen resistance of the paraffin/EVA/paraffin encapsulation layer. Furthermore, paraffin can inhibit the defects and voids of metal electrodes quickly expanding and decaying, which can improve metal electrode stability. Therefore, PSCs encapsulated with EVA and paraffin complex layers can definitely prolong their lifetime compared to PSCs with pure EVA encapsulation.

EXPERIMENTAL SECTION

Materials

$Ni(Ac)_2 \cdot 4H_2O$ (>98%), ethylene glycol monomethyl, ether, and ethanolamine ($NH_2CH_2CH_2OH$) were purchased from Sinopharm Chemical Reagent Co. Ltd. Methylammonium iodide (MAI, 99.5%) [6,6]-phenyl-C_{61}-butyric acid methyl solution ($PC_{61}BM$,>99.9%), and slightly excess lead (ll) iodide (PbI_2, 99%) were purchased from VIZUCHEM. Dimethyl sulphoxide (DMSO, AR 99% GC), chlorobenzene (CB,>99%), and γ-butyrolactone (GBL, AR 99% GC) were purchased from

Aladdin Reagents. The paraffin is a mixture of macromolecular hydrocarbons with a structural formula of C_nH_{2n+2} containing 17 to 35 carbon atoms. The three kinds of paraffin with melting points of 68, 60, and 55°C were purchased from Sinopharm Chemical Reagent Co. Ltd. EVA films were purchased from JCC shanghai.

Device Fabrication

The FTO glasses sequentially cleaned with detergent water, deionized water, acetone, and isopropanol under ultra-sonication were dried in the oven at 120°C and then treated with UV−ozone for 20 min 25 mg $Ni(Ac)_2 \cdot 4H_2O$ was dissolved in ethylene glycol monomethyl (1 ml) with ethanolamine (6 ul) for 4 h at 70°C to form the precursor solution of NiO_x. The NiO_x precursor solution was spin-coated onto FTO glass at 4,500 rpm for 30 s, followed by annealing at 235°C for 45 min in the air to form NiO_x film. The perovskite precursor solution with a 1.3 M concentration was prepared by dissolving methylammonium iodide and slightly excess lead (ll) iodide in a mixed solvent containing 30% dimethyl sulphoxide and 70% γ-butyrolactone. The perovskite precursor solution was dropped on FTO/NiO_x by consecutive two-step spin-coating process at 2000 and 4,000 rpm for 15 and 60 s in the nitrogen-filled glove box. A measure of 0.3 ml of chlorobenzene was dropped as an anti-solvent during the second spin-coating step to replace the DMSO solvent. Then perovskite films were annealed at 100°C for 10 min, and 10 mg/ml $PC_{61}BM$ dissolved in chlorobenzene was spin-coated onto the $CH_3NH_3PbI_3$ layer at 1,200 rpm for 45 s. Finally, 120 nm thick AgAl electrodes were deposited in the thermally evaporated equipment under the vacuum pressure of 5.0×10^{-4} Pa. The device structure of FTO/NiO_x/$CH_3NH_3PbI_3$/$PC_{61}BM$/AgAl is shown in **Supplementary Figure S1**.

Characterization

The cross-section images of samples were measured by field-emission scanning electron microscopy (SEM, Hitachi S-4800). The steady-state photoluminescence (PL) spectra were measured using a fluorescence spectrophotometer (FluoroMax-4, HORIBA Jobin Yvon). The UV-Vis spectrophotometer (U-3900, Hitachi) was used to measure transmission and absorption spectra. The X-ray diffraction (XRD) spectra were obtained from the system of PW3040/60 instrument (Holland Panalytical PRO, Cu Kα radiation of λ with 1.5405 Å). The photocurrent density and voltage (J–V) curves were measured using the Newport solar simulator with AM1.5G and 100 mW/cm^2 illumination.

Encapsulation Process

Three kinds of encapsulating structures were fabricated and the typical encapsulating procedures are shown in **Supplementary Figure S2**. For pure EVA encapsulation, as shown in **Supplementary Figure S2A**, the EVA film was first put onto a glass cover of 1.3 × 1.3 cm size and then heated together on the hot plate at 80°C for 120 s until the EVA film was fully intenerated. Then glass cover with a softened EVA film was put onto the working area of cells and kept squeezing for 30 s to make EVA and a glass cover cling onto cells. The encapsulating
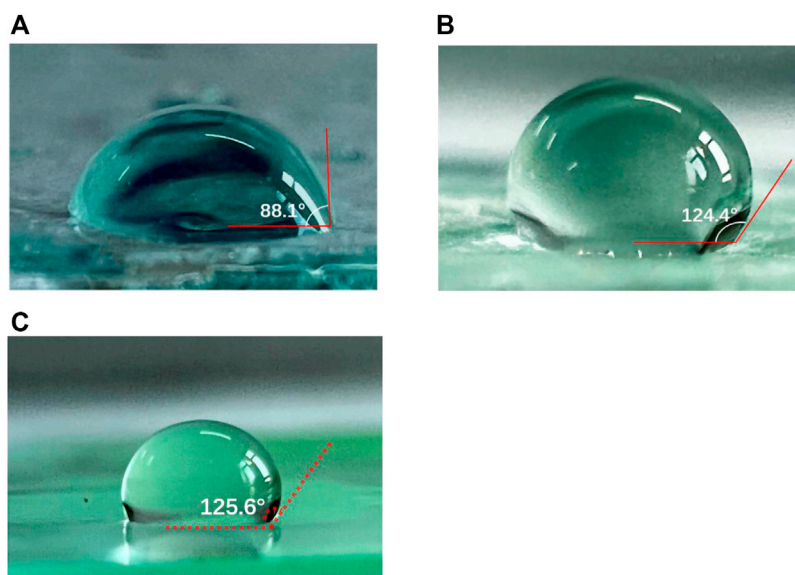
FIGURE 1 | Contact angles of water onto EVA **(A)**, paraffin **(B)** and paraffin/EVA/paraffin films **(C)**.

procedures of pure paraffin are the same as the pure EVA encapsulation, as shown in **Supplementary Figure S2B**.

For encapsulating the structure of paraffin/EVA/paraffin (**Supplementary Figure S2C**), paraffin was first melted onto a glass cover, and then the EVA film was put onto the melted paraffin and softened using the hot plate. The melted paraffin was further dropped onto the EVA film and immersed EVA film at 80°C. Finally, a glass cover with paraffin/EVA/paraffin was quickly squeezed into the work area of cells until completely sticking cells and glass cover.

RESULTS AND DISCUSSIONS

Figure 1 shows the contact angles of water onto EVA、 paraffin films and paraffin/EVA/paraffin films. The contact angles of EVA, paraffin, and paraffin/EVA/paraffin are 88.1°, 124.4°, and 125.6°, respectively. By employing paraffin onto the EVA film, the contact angle of the encapsulated film is obviously increased, indicating that paraffin is an excellent hydrophobic material and helps block moisture immersion as an encapsulating material. Paraffin is a kind of complex organic material with a low molecular weight, which cannot form continuously and dense film due to its low strength and toughness. Paraffin as a non-polar material has chemical inertness, which can avoid chemical interaction with PSCs. The EVA film as a kind of polymer can easily form continuous and consolidated film. The combination strategy of EVA and paraffin as encapsulating complex layers is expected to form continuous and dense hydrophobic composite films by effectively avoiding their weakness and fully employing their advantages.

To demonstrate the encapsulating effects of EVA and paraffin complex films, three kinds of encapsulating structures were fabricated, as shown in **Supplementary Figure S2**. The J–V curves of PSCs before and after encapsulation are shown in **Figure 2**. The similar PCEs of PSCs before and after encapsulation indicate that encapsulating procedures cannot deteriorate the performance of PSCs. The statistical distribution of photovoltaic parameters for PSCs before and after encapsulation further supported that the encapsulating procedures cannot deteriorate the performance of PSCs.

The decay curves of photovoltaic parameters of PSCs under different encapsulation conditions over time are shown in **Figure 3**. The PCEs of PSCs with paraffin/EVA/paraffin and pure EVA encapsulation respectively remained 95 and 45% of original PCEs after aging for 1,000 h under RH 75% and room temperature, indicating that paraffin/EVA/paraffin compared to pure EVA encapsulation layers has better oxygen and moisture resistance. Furthermore, V_{oc} of PSCs with paraffin show better stability compared to FF and Jsc of PSCs, indicating that paraffin directly contacted with the AgAl electrode can inhibit AgAl electrodes decay.

The pinholes and voids of AgAl electrodes cannot completely be avoided during thermally depositing metal electrodes, which can be more easily corroded along with the surrounds of pinholes and voids of metal electrodes (Jiang et al., 2016). Similarly, the edge of metal electrodes for aged cells is easily corroded because Ag clusters on the edge of metal electrode can be easily formed due to the effect of shadow mask (Ding et al., 2021). The melting paraffin during encapsulation has a chance to immerse and fill in pinholes and voids of AgAl electrodes, which helps improve the stability of AgAl electrodes. The optical microscope images of AgAl electrodes of PSCs with different aging times are shown in **Figures 4A–H**. The smooth and bright edges and surface with tiny pinholes and voids can be observed in the pristine AgAl electrode, as shown in **Figures 4A,E**. After aging for 4500 h at RH 75%, many corrosion holes can be observed on the AgAl electrode without encapsulation. The AgAl electrode of PSCs encapsulated
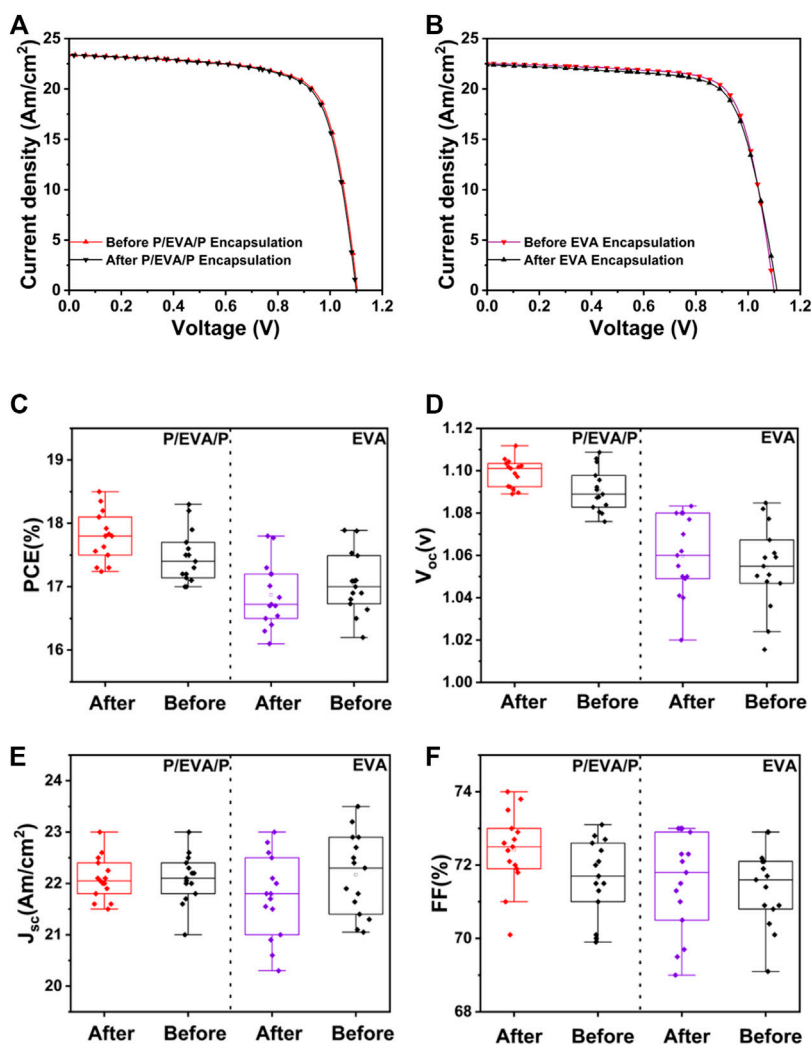
FIGURE 2 | J–V curves of PSCs before and after paraffin/EVA/paraffin/glass **(A)** and EVA/glass **(B)** encapsulation. Statistical deviation from 15 devices of each kind of PSCs for photovoltaic parameters of PCE **(C)**, V_{OC} **(D)**, J_{SC} **(E),** and FF **(F)** before and after encapsulation.

with paraffin/EVA/paraffin layer still cannot be observed the corroded holes aged for 6000 h, as shown in **Figure 4C**. However, the AgAl electrodes of PSCs encapsulated with the pure EVA layer have produced lots of corroded holes after aging for 6000 h compared to the AgAl electrode with paraffin/EVA/paraffin encapsulation. Similarly, the edges of metal electrodes with EVA compared to paraffin/EVA/paraffin encapsulation are more severely corroded. These results indicate that paraffin/EVA/paraffin encapsulation can effectively inhibit metal electrode corrosion and improve the stability of metal electrodes.

The decay performance of PSCs is related to crystallinity and photo-electronic properties of the perovskite layer. The X-ray diffraction (XRD) patterns of perovskite layers with different encapsulation conditions are shown in **Figure 5A**. The (100) main diffraction peak of the perovskite layer is almost disappeared for the control PSCs. The diffraction peak (12.5°) of PbI$_2$ for the perovskite layer encapsulated with the paraffin/EVA/paraffin layer is obviously lower than that of the perovskite

layer encapsulated with the pure EVA layer, indicating that the perovskite layer for paraffin/EVA/paraffin encapsulation is not obviously decayed aging for 5 days. The enhanced steady PL (**Figure 5B**) and absorption intensity (**Figure 5C**) of perovskite layers with paraffin/EVA/paraffin encapsulation compared to pure EVA encapsulation supported that paraffin/EVA/paraffin has better encapsulation effects. The scanning electron microscope (SEM) cross-section images of PSCs encapsulated with EVA and paraffin/EVA/paraffin are shown in **Supplementary Figure S3**. PSCs with paraffin/EVA/paraffin show clearly the cross-section of perovskite layer aged for 500 h, further demonstrating that using paraffin/EVA/paraffin encapsulation method can well inhibit the decay of perovskite layers, which is consistent with PCEs decay trend of PSCs.

The physical properties of paraffin are related to molecular weight, which would change its melting point and the encapsulation effect. The three kinds of paraffin with different melting points (55, 60, and 68°C) were employed to encapsulate
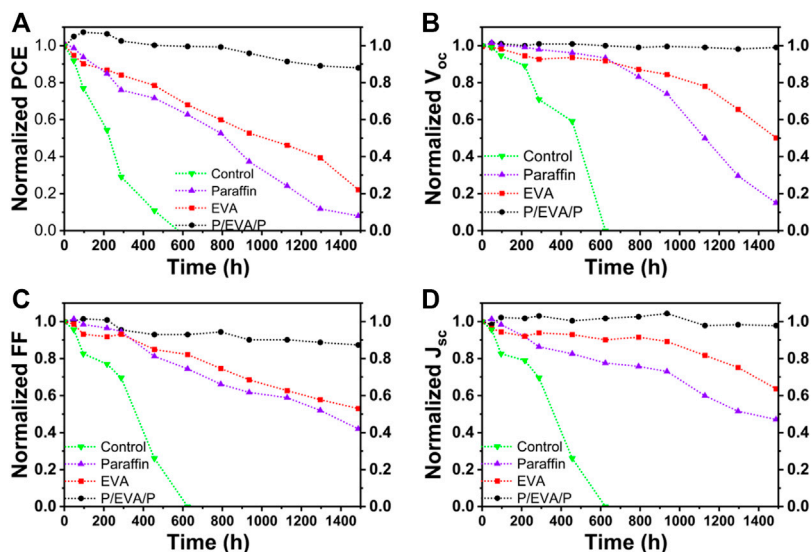
FIGURE 3 | Evolution of photovoltaic parameters of PSCs with different encapsulated structures for normalized PCEs **(A)**, V_{OC} **(B)**, FF**(C),** and J_{SC} **(D)** aged for RH 75% and room temperature. Encapsulated structures are EVA, paraffin and paraffin/EVA/paraffin films, respectively.
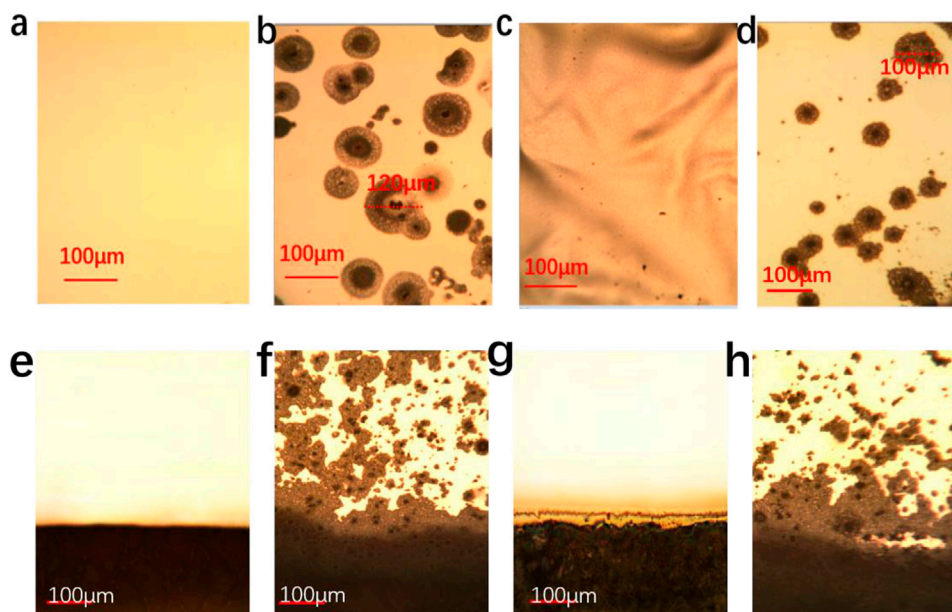

FIGURE 4 | Metallurgical microscope images of middle **(A)** and edge **(E)** of pristine AgAl electrodes, middle **(B)** and edge **(F)** of AgAl electrodes without encapsulation, middle **(C)** and edge **(G)** of AgAl electrodes with paraffin/EVA/paraffin encapsulation, middle **(D)** and edge **(H)** of AgAl electrodes with pure EVA encapsulation aged for RH 75% and room temperature.

PSCs. The paraffin/EVA/paraffin encapsulated PSCs with different melting points were aged under different conditions, as shown in **Figure 6**. PSCs encapsulated with 68°C paraffin/EVA/paraffin remaining 95% of their initial PCEs aged for 1,000 h at RH 75% and room temperature condition, which show superior stability compared to 55 and 60°C paraffin/

EVA/paraffin encapsulated PSCs, indicating that the high melting point of paraffin with larger molecular weight helps improve moisture resistance.

The superior thermal and moisture stability of paraffin/EVA/paraffin with 68°C melting point paraffin compared to 60 and 55°C paraffin can further be demonstrated through aging at 60°C
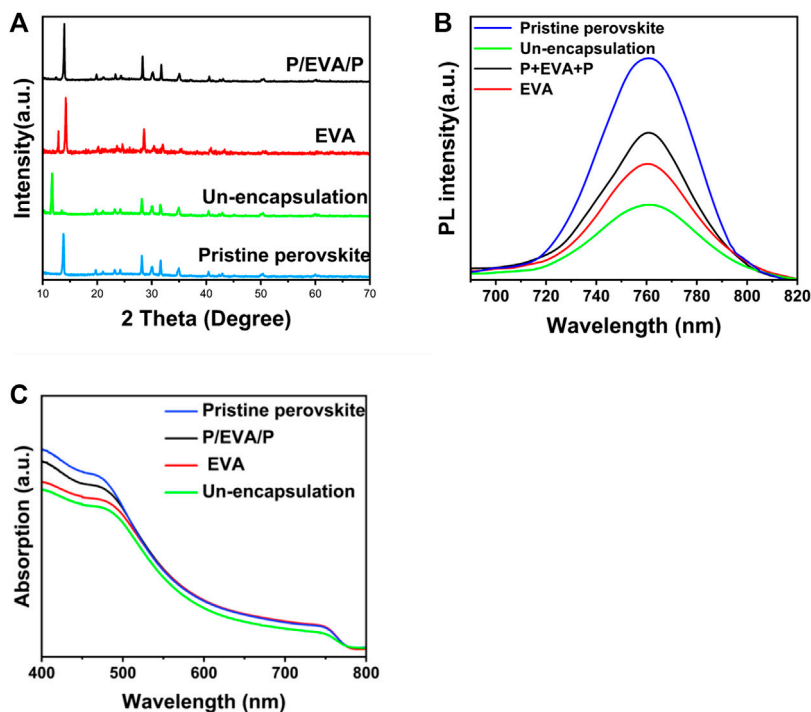
FIGURE 5 | Evolution of XRD patterns **(A)**, steady-state PL spectra **(B)** and UV-vis absorption spectra **(C)** for perovskite films with different encapsulation structures aged for 5 days at RH 75% and room temperature.
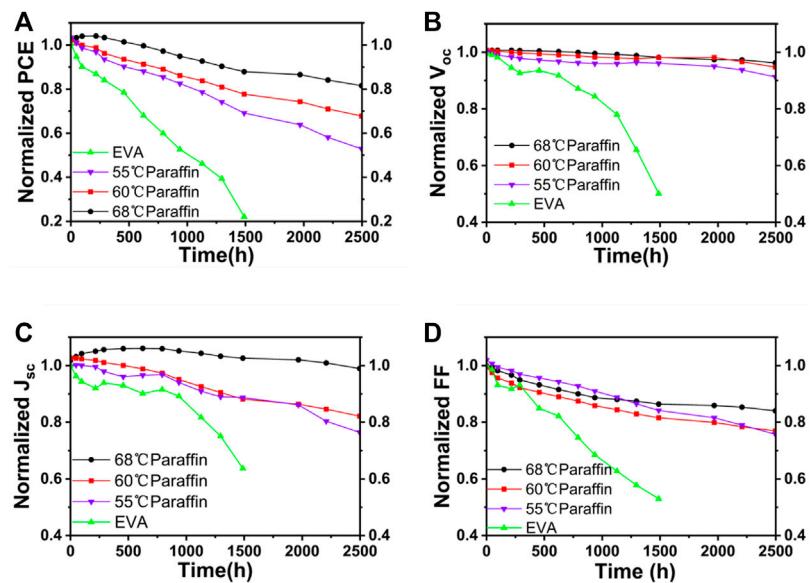

FIGURE 6 | Long-term stability of PSCs encapsulated with paraffin/EVA/paraffin with different melting points paraffin at 75% RH and room temperature **(A)**. Evolution of photovoltaic parameters of PSC encapsulated by different melting points paraffin for V_{OC} **(B)**, J_{SC} **(C)** and FF **(D)**.

and RH 85% condition, as shown in **Figure 7**. PSCs with 68°C melting point paraffin/EVA/paraffin retain 90% of their initial PCEs aging for 1,000 h. Furthermore, the V_{oc} values of PSCs within 1,000 h show amazing stability, as shown in **Figure 7B**,

indicating that the decay of the AgAl electrode can be well inhibited using high melting point paraffin protection.

To strictly test the performance of PSCs under extreme weather conditions, PSCs with different encapsulation
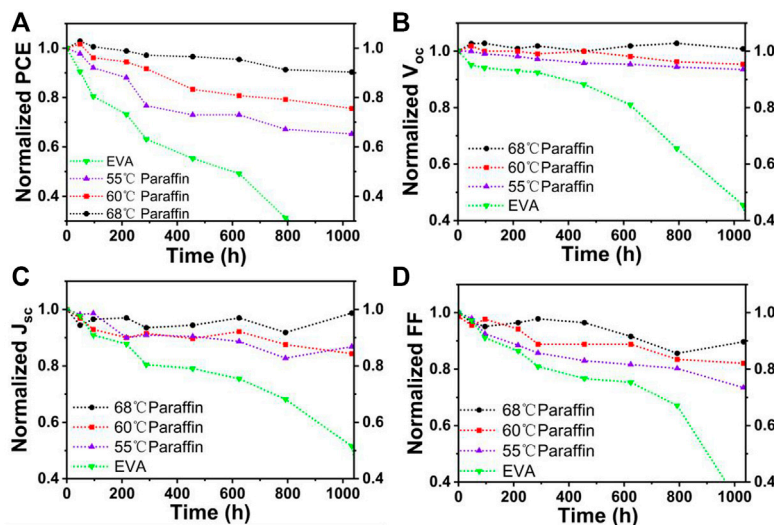
FIGURE 7 | Long-term stability of PSCs encapsulated with different melting point paraffin in 85% humidity and 60°C. Normalized PCE (A), V_{oc} (B), J_{SC} (C), and FF (D) evolution of encapsulated PSCs with time.
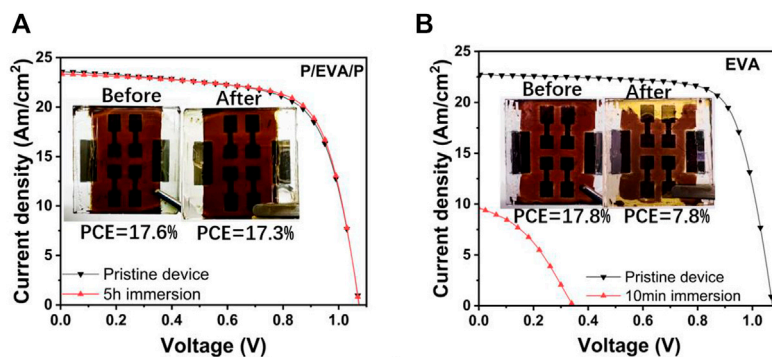

FIGURE 8 | J–V curves and photos of PSCs with paraffin/EVA/paraffin before and after immersing in water for 5 h (A). J–V curves and photos of PSCs with EVA before and after immersing in water for 10 min (B).

structures were directly immersed in water. The J–V curves of PSCs with two kinds of encapsulated structures before and after immersing into water are shown in **Figure 8**. The melting point of paraffin is 68°C. PSCs with the pure EVA encapsulated layer were rapidly decreased to 8% (PCEs) after immersing into water for only 10 min. However, PSCs with the paraffin/EVA/paraffin encapsulation layer almost retained the same constant initial values, indicating that paraffin/EVA/paraffin encapsulated structures show excellent water-resistance, which is far superior to that of pure EVA encapsulation layer.

CONCLUSION

Paraffin/EVA/paraffin and pure EVA encapsulating structures have carefully been investigated and PSCs

encapsulated with paraffin/EVA/paraffin show superior encapsulation performance. PSCs with paraffin/EVA/paraffin encapsulation retained 95% aged for 1,000 h at RH 75% and remained 98% of initial PCEs after immersing into water for 5 h. The paraffin of high melting point at 68°C shows better encapsulation than low melting point paraffin, indicating that the high molecular weight of paraffin is important for improving the encapsulation performance of PSCs. Furthermore, paraffin can inhibit defects, voids, and edges of metal electrodes quickly expand and decay, which help improve the stability of V_{oc} compared to the pure EVA encapsulating layer. Therefore, the combination strategy of EVA and paraffin as encapsulating complex layers is an effective technology to form continuous and dense hydrophobic composite films,

which can effectively avoid their weakness and fully employ their advantages.

DATA AVAILABILITY STATEMENT

The raw data supporting the conclusions of this article will be made available by the authors, without undue reservation.

AUTHOR CONTRIBUTIONS

BL: conceptualization, investigation, writing-original draft, and data curation. XZ: data curation and investigation. HC: data curation and formal analysis. RC: validation and formal analysis. NH: methodology and conceptualization. LC: validation. PF: formal analysis. XC: supervision, writing–review and editing.

FUNDING

SUPPLEMENTARY MATERIAL

The Supplementary Material for this article can be found online at: https://www.frontiersin.org/articles/10.3389/fmats.2022.892657/full#supplementary-material

REFERENCES

Alkan, C., Sarı, A., and Karaipekli, A. (2011). Preparation, thermal Properties and thermal Reliability of Microencapsulated N-Eicosane as Novel Phase Change Material for thermal Energy Storage. *Energ. Convers. Manag.* 52, 687–692. doi:10.1016/j.enconman.2010.07.047

Asghar, M. I., Zhang, J., Wang, H., and Lund, P. D. (2017). Device Stability of Perovskite Solar Cells - A Review. *Renew. Sust. Energ. Rev.* 77, 131–146. doi:10.1016/j.rser.2017.04.003

Babaei, A., Zanoni, K. P. S., Gil-Escrig, L., Pérez-del-Rey, D., Boix, P. P., Sessolo, M., et al. (2020). Efficient Vacuum Deposited P-I-N Perovskite Solar Cells by Front Contact Optimization. *Front. Chem.* 7, 936. doi:10.3389/fchem.2019.00936

Chen, X., Zhou, H., and Wang, H. (2021a). 2D/3D Halide Perovskites for Optoelectronic Devices. *Front. Chem.* 9, 715157. doi:10.3389/fchem.2021.715157

Chen, Z., He, P., Wu, D., Chen, C., Mujahid, M., Li, Y., et al. (2021b). Processing and Preparation Method for High-Quality Opto-Electronic Perovskite Film. *Front. Mater.* 8, 723169. doi:10.3389/fmats.2021.723169

Corsini, F., and Griffini, G. (2020). Recent Progress in Encapsulation Strategies to Enhance the Stability of Organometal Halide Perovskite Solar Cells. *J. Phys. Energ.* 2, 031002. doi:10.1088/2515-7655/ab8774

Ding, C., Yin, L., Zhang, L., Huang, R., Fan, S., Luo, Q., et al. (2021). Revealing the Mechanism behind the Catastrophic Failure of N-i-p Type Perovskite Solar Cells under Operating Conditions and How to Suppress it. *Adv. Funct. Mater.* 31, 2103820. doi:10.1002/adfm.202103820

Filip, M. R., Eperon, G. E., Snaith, H. J., and Giustino, F. (2014). Steric Engineering of Metal-Halide Perovskites with Tunable Optical Band Gaps. *Nat. Commun.* 5, 5757. doi:10.1038/ncomms6757

Fu, Z., Xu, M., Sheng, Y., Yan, Z., Meng, J., Tong, C., et al. (2019). Encapsulation of Printable Mesoscopic Perovskite Solar Cells Enables High Temperature and Long-Term Outdoor Stability. *Adv. Funct. Mater.* 29, 1809129. doi:10.1002/adfm.201809129

Jeon, N. J., Na, H., Jung, E. H., Yang, T.-Y., Lee, Y. G., Kim, G., et al. (2018). A Fluorene-Terminated Hole-Transporting Material for Highly Efficient and Stable Perovskite Solar Cells. *Nat. Energ.* 3, 682–689. doi:10.1038/s41560-018-0200-6

Jiang, Z., Chen, X., Lin, X., Jia, X., Wang, J., Pan, L., et al. (2016). Amazing Stable Open-Circuit Voltage in Perovskite Solar Cells Using AgAl alloy Electrode. *Solar Energ. Mater. Solar Cell* 146, 35–43. doi:10.1016/j.solmat.2015.11.026

Kempe, M. D., Jorgensen, G. J., Terwilliger, K. M., McMahon, T. J., Kennedy, C. E., and Borek, T. T. (2007). Acetic Acid Production and Glass Transition Concerns with Ethylene-Vinyl Acetate Used in Photovoltaic Devices. *Solar Energ. Mater. Solar Cell* 91, 315–329. doi:10.1016/j.solmat.2006.10.009

Kim, N., Potscavage, W. J., Sundaramoothi, A., Henderson, C., Kippelen, B., and Graham, S. (2012). A Correlation Study between Barrier Film Performance and Shelf Lifetime of Encapsulated Organic Solar Cells. *Solar Energ. Mater. Solar Cell* 101, 140–146. doi:10.1016/j.solmat.2012.02.002

Krupa, I., Miková, G., and Luyt, A. S. (2007). Phase Change Materials Based on Low-Density Polyethylene/paraffin Wax Blends. *Eur. Polym. J.* 43, 4695–4705. doi:10.1016/j.eurpolymj.2007.08.022

Li, J., Xia, R., Qi, W., Zhou, X., Cheng, J., Chen, Y., et al. (2021). Encapsulation of Perovskite Solar Cells for Enhanced Stability: Structures, Materials and Characterization. *J. Power Sourc.* 485, 229313. doi:10.1016/j.jpowsour.2020.229313

Lin, C. (2020). Stabilizing Organic-Inorganic Lead Halide Perovskite Solar Cells with Efficiency beyond 20. *Front. Chem.* 8, 592. doi:10.3389/fchem.2020.00592

Liu, D., and Kelly, T. L. (2014). Perovskite Solar Cells with a Planar Heterojunction Structure Prepared Using Room-Temperature Solution Processing Techniques. *Nat. Photon* 8, 133–138. doi:10.1038/nphoton.2013.342

Liu, X., Tan, X., Liu, Z., Ye, H., Sun, B., Shi, T., et al. (2019). Boosting the Efficiency of Carbon-Based Planar CsPbBr3 Perovskite Solar Cells by a Modified Multistep Spin-Coating Technique and Interface Engineering. *Nano Energy* 56, 184–195. doi:10.1016/j.nanoen.2018.11.053

Ma, S., Yuan, G., Zhang, Y., Yang, N., Li, Y., and Chen, Q. (2022). Development of Encapsulation Strategies towards the Commercialization of Perovskite Solar Cells. *Energy Environ. Sci.* 151039, 13–55. doi:10.1039/D1EE02882K

Mazumdar, S., Zhao, Y., and Zhang, X. (2021). Stability of Perovskite Solar Cells: Degradation Mechanisms and Remedies. *Front.Electron.* 2, 712785. doi:10.3389/felec.2021.712785

Min, H., Lee, D. Y., Kim, J., Kim, G., Lee, K. S., Kim, J., et al. (2021). Perovskite Solar Cells with Atomically Coherent Interlayers on SnO2 Electrodes. *Nature* 598, 444–450. doi:10.1038/s41586-021-03964-8

Mohammadi, M., Gholipour, S., Malekshahi Byranvand, M., Abdi, Y., Taghavinia, N., and Saliba, M. (2021). Encapsulation Strategies for Highly Stable Perovskite Solar Cells under Severe Stress Testing: Damp Heat, Freezing, and Outdoor Illumination Conditions. *ACS Appl. Mater. Inter.* 13, 45455–45464. doi:10.1021/acsami.1c11628

Ponseca, C. S., Savenije, T. J., Abdellah, M., Zheng, K., Yartsev, A., Pascher, T., et al. (2014). Organometal Halide Perovskite Solar Cell Materials Rationalized: Ultrafast Charge Generation, High and Microsecond-Long Balanced Mobilities, and Slow Recombination. *J. Am. Chem. Soc.* 136, 5189–5192. doi:10.1021/ja412583t

Raman, R. K., Gurusamy Thangavelu, S. A., Venkataraj, S., and Krishnamoorthy, A. (2021). Materials, Methods and Strategies for Encapsulation of Perovskite Solar Cells: From Past to Present. *Renew. Sust. Energ. Rev.* 151, 111608. doi:10.1016/j.rser.2021.111608

Ramos, F. J., Maindron, T., Béchu, S., Rebai, A., Frégnaux, M., Bouttemy, M., et al. (2018). Versatile Perovskite Solar Cell Encapsulation by Low-Temperature ALD-Al2O3 with Long-Term Stability Improvement. *Sust. Energ. Fuels* 2, 2468–2479. doi:10.1039/C8SE00282G

Shi, L., Young, T. L., Kim, J., Sheng, Y., Wang, L., Chen, Y., et al. (2017). Accelerated Lifetime Testing of Organic-Inorganic Perovskite Solar Cells Encapsulated by

Polyisobutylene. *ACS Appl. Mater. Inter.* 9, 25073–25081. doi:10.1021/acsami.7b07625

Singh, R., Ghosh, S., Subbiah, A. S., Mahuli, N., and Sarkar, S. K. (2020). ALD Al2O3 on Hybrid Perovskite Solar Cells: Unveiling the Growth Mechanism and Long-Term Stability. *Solar Energ. Mater. Solar Cell* 205, 110289. doi:10.1016/j.solmat.2019.110289

Stranks, S. D., Eperon, G. E., Grancini, G., Menelaou, C., Alcocer, M. J. P., Leijtens, T., et al. (2013). Electron-Hole Diffusion Lengths Exceeding 1 Micrometer in an Organometal Trihalide Perovskite Absorber. *Science* 342, 341–344. doi:10.1126/science.1243982

Tiep, N. H., Ku, Z., and Fan, H. J. (2016). Recent Advances in Improving the Stability of Perovskite Solar Cells. *Adv. Energ. Mater.* 6, 1501420. doi:10.1002/aenm.201501420

Uddin, A., Upama, M., Yi, H., and Duan, L. (2019). Encapsulation of Organic and Perovskite Solar Cells: A Review. *Coatings* 9, 65. doi:10.3390/coatings9020065

van der Stam, W., Geuchies, J. J., Altantzis, T., van den Bos, K. H. W., Meeldijk, J. D., Van Aert, S., et al. (2017). Highly Emissive Divalent-Ion-Doped Colloidal CsPb1-xMxBr3 Perovskite Nanocrystals through Cation Exchange. *J. Am. Chem. Soc.* 139, 4087–4097. doi:10.1021/jacs.6b13079

Xing, G., Mathews, N., Sun, S., Lim, S. S., Lam, Y. M., Grätzel, M., et al. (2013). Long-Range Balanced Electron- and Hole-Transport Lengths in Organic-Inorganic CH 3 NH 3 PbI 3. *Science* 342, 344–347. doi:10.1126/science.1243167

Zardetto, V., Williams, B. L., Perrotta, A., Di Giacomo, F., Verheijen, M. A., Andriessen, R., et al. (2017). Atomic Layer Deposition for Perovskite Solar Cells: Research Status, Opportunities and Challenges. *Sust. Energ. Fuels* 1, 30–55. doi:10.1039/C6SE00076B

Zhang, J., Mao, W., Hou, X., Duan, J., Zhou, J., Huang, S., et al. (2018). Solution-processed Sr-Doped NiOx as Hole Transport Layer for Efficient and Stable Perovskite Solar Cells. *Solar Energy* 174, 1133–1141. doi:10.1016/j.solener.2018.10.004

Zheng, J., Chen, J., Ouyang, D., Huang, Z., He, X., Kim, J., et al. (2020). Critical Role of Functional Groups in Defect Passivation and Energy Band Modulation in Efficient and Stable Inverted Perovskite Solar Cells Exceeding 21% Efficiency. *ACS Appl. Mater. Inter.* 12, 57165–57173. doi:10.1021/acsami.0c18862